EPITAXIALLY-ENCAPSULATED QUAD MASS RESONATOR WITH SHAPED COMB FINGERS FOR FREQUENCY TUNING

Parsa Taheri-Tehrani[1], Martial Defoort[1], Yunhan Chen[2], Ian Flader[2], Dongsuk D. Shin[2], Thomas W. Kenny[2], and David A. Horsley[1]
[1]University of California Davis, Davis, CA, USA
[2]Stanford University, Stanford, CA, USA

ABSTRACT

We present an epitaxially-encapsulated 2x2mm^2 quad-mass resonator (QMR) with shaped comb fingers for frequency tuning. While shaped electrodes have been used for frequency tuning of linear resonators, the device studied here has very high quality factor (Q=100,000) resulting in a very narrowband resonance which, without the shaped electrodes, results in undesirable nonlinear behavior such as amplitude-frequency dependence and instability of the oscillator loop at large amplitudes. We demonstrate that through the shaped comb finger design, both frequency tuning (over 90Hz) and large amplitude oscillation (1.25 µm amplitude, a factor of 100 compared to performance without the shaped electrodes) are possible. Furthermore, we demonstrate how critical dimension loss in the fabrication process can change the shape of the designed shaped finger and introduce electrostatic stiffness hardening.

INTRODUCTION

In MEMS resonators used in applications such as vibratory gyroscopes [1,2] and timing oscillators [3], high signal-to-noise ratio can be achieved through having large vibration amplitude and high quality factor, Q. Conversely, high-Q resonators are very sensitive to amplitude-dependent nonlinearities which cause a variety of undesired effects such as bifurcation in the frequency response, unstable behavior and amplitude-induced frequency fluctuations. In parallel, having a substantial control of the resonance frequency is mandatory in many MEMS resonator applications. Implementing both frequency tuning and achieving large linear oscillation is a challenge for electrostatically actuated MEMS. Using parallel-plate electrodes for frequency tuning is well-known for a variety of resonators [1,2,4]; however, this type of electrode creates nonlinearity and the electrode gap limits the oscillation amplitude or requires high voltage if the electrode gap is large.

Although cancelling nonlinearity has been illustrated [1,5,6], it has limited success [1,7,8]. Using good mechanical design and using comb fingers (rather than parallel-plate electrodes) one can avoid nonlinear oscillation, however; to implement frequency tuning, comb fingers with a shaped profile are needed [9,10]. Previous demonstrations of shaped comb fingers were on low quality-factor devices with low resonance frequencies, because earlier shaped combs were not capable of generating enough voltage-controlled stiffness to tune a stiff, high-frequency device.

Here, we present a quad-mass resonator (QMR), illustrated in Fig. 1(a), having two vibration modes illustrated in Fig. 1(b). This device has four proof masses (M) and sixteen drive frames (m). Electrostatic drive, sense, and tuning of the resonator is done through the drive frames. The QMR device can potentially be used as a gyroscope [1,11]. The device is fabricated from a 20 µm single-crystal silicon layer, and it is epitaxially encapsulated at a very low pressure (1 Pa) which results in a quality factor of 100,000 [12], a factor of 6 greater than [9]. By using comb fingers for actuation and transduction of the motion, the resonator can be driven to a peak amplitude of 1.25 µm in the linear regime without passing the bifurcation point, an amplitude that is 10 times greater than that of a similar device presented in [1], which used parallel-plate electrodes. We demonstrate shaped combs which achieve a 90 Hz frequency tuning range at 40V tuning voltage. Achieving this wide tuning range on a stiff resonator operating at 52 kHz is possible using shaped comb finger electrodes with a sub-micron (0.7µm) gap.

RESONATOR DYNAMICS

The resonator dynamics are described by the Duffing equation:

$$\ddot{u} + \frac{\omega_n}{Q}\dot{u} + \omega_n^2 u + \frac{k_3}{m}u^3 = F \qquad (1)$$

where u represents displacement, ω_n is the natural frequency, Q is the quality factor, m the modal mass, and k_3 is the stiffness coefficient corresponding to the cubic nonlinearity of the resonator. The sign of k_3 determines whether nonlinear spring-softening (negative), or nonlinear spring-hardening (positive) is present. Amplitude-frequency (A-f) dependence, which arises from

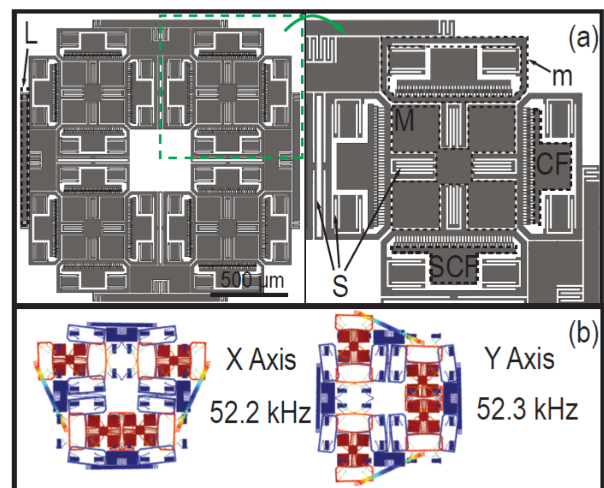

Fig. 1: Layout and vibration modes of the 2 mm square QMR. (a) Device layout showing M: proof mass, m: drive frames, L: lever, CF: comb fingers, SCF: shaped comb fingers, and S: springs. (b) Mode shapes and natural frequencies of the two modes.

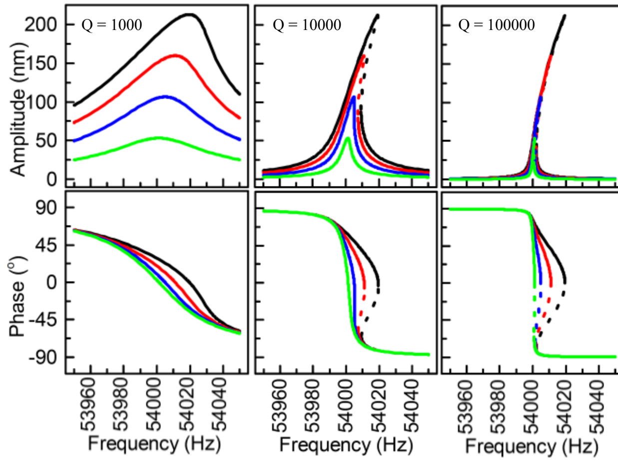

Fig. 2: Simulated QMR frequency responses for three different values of Q. Above the bifurcation threshold, there are branches that are open-loop unstable (dashed lines). The bifurcation threshold occurs at lower amplitude if the quality factor is higher.

nonlinearity, is not dependent on the quality factor of the resonator but having a larger quality factor will make the nonlinearity more visible as the bifurcation amplitude is dependent on the bandwidth of the resonator [13].

Simulations of the Duffing oscillator's frequency response were conducted using parameters similar to those of the QMR presented in [1,14]. In these simulations, $k_3 = 0.5\times10^{14}$ (N/m^3), typical for the QMR device. The simulation results are plotted in Fig. 2 for three different quality factors. The figure shows that as the quality factor increases, the bifurcation amplitude decreases. Although the nonlinearity's value does not change in these simulations, higher quality factor makes the resonator more sensitive to nonlinearities. As a result, it is more challenging to achieve large amplitude oscillation in a high quality factor device than in a low quality factor device.

SHAPED COMB FINGER DESIGN

Standard design

The ideal profile of a shaped electrode to produce a linear spring constant was described in [10,15]. This profile is parametrized by the following equation:

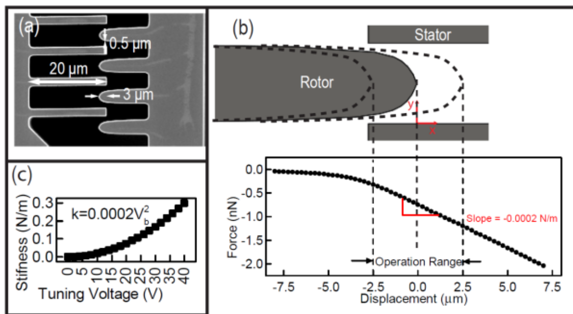

Fig. 3: Shaped comb finger design. (a) SEM image of the shaped comb finger illustrating dimensions of the design. (b) Results of FEM simulations of a single shaped comb finger showing a linear operating range of 5 µm (peak-to-peak) displacement, creating a stiffness of 0.0002 N/m for a tuning voltage of 1V for one shaped comb finger. (c) Quadratic dependency of the stiffness on tuning voltage.

$$[x_i, y_i(x_i)] = [x_i, \frac{g_0}{1 + x_i / x_0}] \quad (2)$$

where g_0 is the distance between the centerline of the shaped comb finger and the wall of a straight comb finger and x_0 is a parameter which controls the taper. By decreasing x_0, the stiffness that is produced by shaped comb finger will increase. The limitation in decreasing x_0 is the minimum gap between the shaped finger and the straight finger. For a fixed minimum gap, there is a trade-off between the linear operating range and the stiffness created by the shaped finger. Because high frequency devices with high stiffness requires large electrostatic negative stiffness to obtain significant frequency tuning, and, in parallel, to achieve large displacement operation range, one should use a fabrication process which allows sub-micron minimum gap.

The designed shaped finger is illustrated in Fig. 3(a) with a minimum gap of 0.5 µm and an engagement length of 3 µm ($x_0 = 0.75$ µm, $g_0 = 2.5$ µm). This design allows a linear operating range of 5 µm (peak-to-peak), as presented in Fig. 3(b). Fig. 3(c) illustrates the expected voltage dependence of the linear stiffness softening, predicting 0.0002 N/m at 1V for one shaped finger. The QMR design has a total of 164 shaped comb fingers per vibration axis, resulting in a theoretical maximum tuning range of 550 Hz at 40V. Later in the paper, we show how fabrication variations modify the tuning characteristic.

Effect of fabrication imperfections

The etching processes used in MEMS fabrication result in reduction in the size of critical dimensions (CD), a phenomenon commonly known as CD loss. This CD loss will change the profile of the shaped finger. Generally a parametric function can be developed to show the profile of the shaped comb finger after fabrication:

$$[x_f(x_i), y_f(x_i)] = [x_i + \frac{O_x}{\sqrt{1+\left(\frac{1}{dy_i/dx_i}\right)^2}}, y_i(x_i) - \frac{O_y}{\sqrt{1+\left(\frac{dy_i}{dx_i}\right)^2}}] \quad (3)$$

where $[x_f, y_f]$ are the coordinates of the final profile, O_x and O_y are CD loss values (negative values) for the x and y directions, and dy_i/dx_i is the derivative of the original profile of the shaped-comb finger.

Fig. 4 (a) shows how an isotropic CD loss (here of 0.25 µm) will change the profile of the shaped comb finger. Fig. 4 (b) shows the force-displacement curve of the shaped comb finger as-drawn and as-fabricated. The slope of the curve, which determines the electrostatic spring-constant, is reduced due to the increase in the gap between comb fingers. In addition, the curve is nonlinear. While an isotropic CD loss results in nonlinear softening at large amplitudes, nonlinear stiffening can also occur from anisotropic changes in the profile.

EXPERIMENTS

Fig. 5 shows a block-diagram of the QMR operation and a schematic of the electrode configuration of the resonator. Two sets of straight comb-finger electrodes are used for single-ended drive of the X-axis resonance mode, and two sets of straight comb-finger electrodes are used for differential sense of this mode. This figure also illustrates

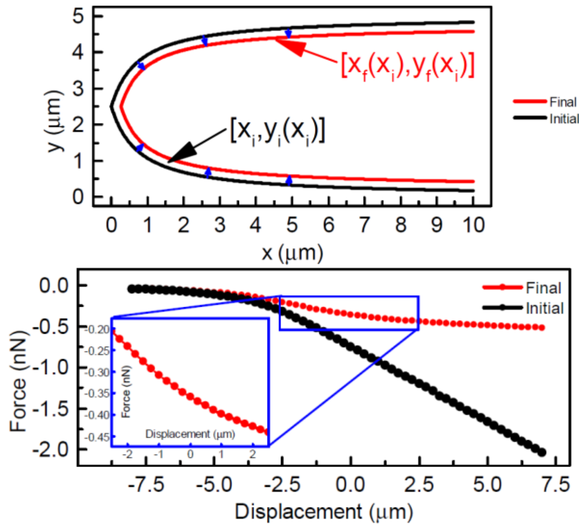

Fig. 4: Effect of CD loss on the profile of the shaped electrode. (a) Profile of the shaped electrode as drawn (red), and as-fabricated (black) after an isotropic CD loss of 0.25 μm. (b) Force-displacement curve of the initial profile (black) and after CD loss (red). The final curve has lower slope (spring-constant) and is nonlinear.

a block diagram of the test setup used to characterize the performance of the QMR. The device is placed on a PCB along with analog front-end amplifiers and the sense signals are processed in lock-in-amplifier (HF2LI, Zurich Instruments AG). A PLL (phase-locked loop) within the lock-in amplifier is used to force the QMR into oscillation with a desired phase shift between input and output. The proof-mass bias voltage and tuning voltages are set through the lock-in-amplifier's analog outputs as well.

Frequency tuning experiments were conducted using a 20V bias applied to the QMR proof-mass and -20 V to +20 V applied to the tuning electrodes, resulting in a net tuning voltage range from 0 to 40V. The results, shown in Fig. 6, demonstrate a 90 Hz tuning range. Frequency response measurements were conducted at four different driving amplitudes selected to exhibit different *A-f* dependence. The differential sensing scheme and high *Q*-factor resulted in a negligible amount of capacitive feed-through, and the measured response, shown in Fig. 7, clearly shows the device's resonance behavior. Note that at large amplitudes, each of the curves exhibits multiple amplitude branches as

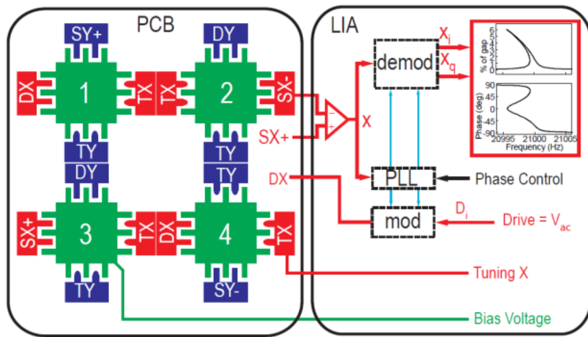

Fig. 5: Block diagram of setup for QMR testing and a schematic showing the electrode layout of the device. Two electrodes are used for single-ended drive (DX), two electrodes for differential sense (SX+/-), and four shaped electrodes are used for frequency tuning (TX).

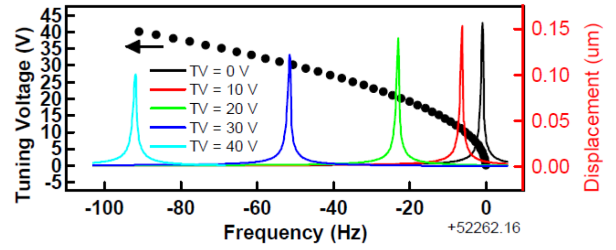

Fig. 6: Measured tuning range of the resonator for tuning voltages from 0-40 V, showing a range of 90 Hz, with four sample frequency sweeps.

predicted by the models shown in Fig. 2, some of which are open-loop unstable [16]. The response at each branch was measured by locking the PLL to the specific phase of oscillation corresponding to the desired amplitude branch, a technique which allows stable oscillation to be achieved at all branches [17].

Fig. 8 (a) shows the amplitude-frequency relationship for different bias voltage, also known as the backbone curve. These data are measured by locking the phase of the oscillator to -90º which corresponds to the maximum amplitude at each drive voltage. The figure shows that the back-bone curve is independent of the bias voltage.

Fig. 8 (b), on the other hand, shows the dependence of *A-f* on the tuning voltage. As suggested in the previous section, shaped comb fingers can exhibit nonlinearity due to the change in profile resulting from CD loss. The measurements presented here show a tuning voltage dependent stiffness-hardening that increases with the tuning voltage. Also as presented in [10], some comb-finger profiles could introduce electrostatic hardening. In our case, preliminary simulations of the shaped fingers using Eq. (3) show that a difference in CD loss rate in the x and y directions ($O_x \neq O_y$) will result in electrostatic stiffness-hardening.

To solve the problem of CD loss, we suggest that a modified profile could be used to draw the layout for the shaped comb finger. If the expected CD loss of the fabrication process is known, one can use Eq. (3) with positive values for O_x and O_y to compute a modified profile.

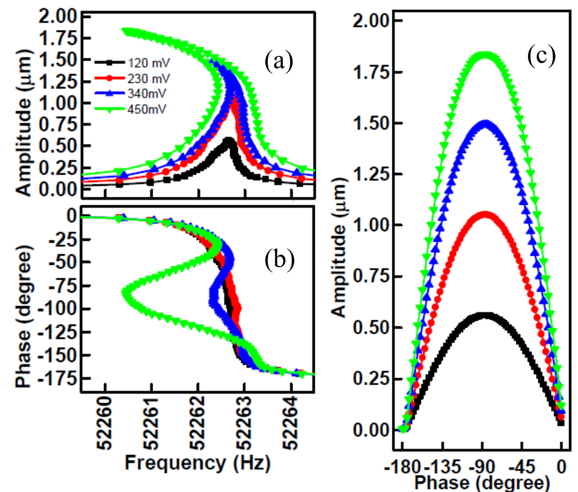

Fig. 7: Nonlinear resonance (a) Amplitude versus frequency measurements showing a linear range of 1.25 μm (2.5 μm peak-to-peak). (b) Measured phase of the oscillation (c) Amplitude-phase relation for the same measurements.

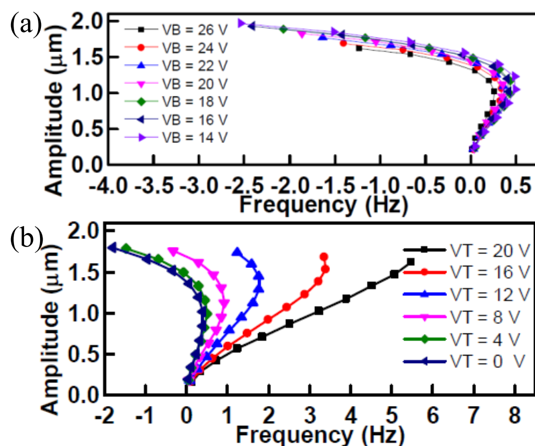

Fig. 8: Duffing backbone curves measured to illustrate that the A-f dependence does not depend on bias voltage (a), and but does depend on the tuning voltage (b).

After fabrication, one can expect to achieve an ideal profile (*i.e.* Eq. (2)) for the shaped finger. Note that Eq. (3) is a general equation and can be used for any profile as long as the function of the profile is known.

CONCLUSION

In this paper we have shown a successful demonstration of shaped comb fingers for frequency tuning of high quality factor devices in episeal fabrication process. We have shown how CD loss can introduce nonlinearity in the shaped finger stiffness and have proposed a method to solve this issue. The results presented in this paper can be used to provide guidelines for design of shaped comb fingers.

ACKNOWLEDGEMENTS

The authors thank Professor Bernhard Boser and his group at the University of California at Berkeley for the initial resonator design. The Stanford portion of this work was supported by a DARPA grant from the PRIGM program, managed by Dr. Robert Lutwak.

REFERENCES

[1] P. Taheri-Tehrani *et al.*, "Epitaxially-encapsulated quad mass gyroscope with nonlinearity compensation," in *2016 IEEE 29th International Conference on Micro Electro Mechanical Systems (MEMS)*, 2016, pp. 966–969.

[2] S. Sonmezoglu, S. E. Alper, and T. Akin, "An Automatically Mode-Matched MEMS Gyroscope With Wide and Tunable Bandwidth," *J. Microelectromechanical Syst.*, vol. 23, no. 2, pp. 284–297, Apr. 2014.

[3] A. Hajimiri and T. H. Lee, "A general theory of phase noise in electrical oscillators," *IEEE J. Solid-State Circuits*, vol. 33, no. 2, pp. 179–194, Feb. 1998.

[4] B. J. Gallacher, J. Hedley, J. S. Burdess, A. J. Harris, A. Rickard, and D. O. King, "Electrostatic correction of structural imperfections present in a microring gyroscope," *J. Microelectromechanical Syst.*, vol. 14, no. 2, pp. 221–234, Apr. 2005.

[5] N. Kacem, S. Hentz, D. Pinto, B. Reig, and V. Nguyen, "Nonlinear dynamics of nanomechanical beam resonators: improving the performance of NEMS-based sensors," *Nanotechnology*, vol. 20, no. 27, p. 275501, 2009.

[6] E. Tatar, T. Mukherjee, and G. K. Fedder, "Nonlinearity tuning and its effects on the performance of a MEMS gyroscope," in *2015 Transducers - 2015 18th International Conference on Solid-State Sensors, Actuators and Microsystems (TRANSDUCERS)*, 2015, pp. 1133–1136.

[7] N. Kacem and S. Hentz, "Bifurcation topology tuning of a mixed behavior in nonlinear micromechanical resonators," *Appl. Phys. Lett.*, vol. 95, no. 18, p. 183104, Nov. 2009.

[8] J. Juillard, A. Bonnoit, E. Avignon, S. Hentz, and E. Colinet, "Large amplitude dynamics of micro-/nanomechanical resonators actuated with electrostatic pulses," *J. Appl. Phys.*, vol. 107, no. 1, p. 14907, Jan. 2010.

[9] C. Guo and G. K. Fedder, "A quadratic-shaped-finger comb parametric resonator," *J. Micromechanics Microengineering*, vol. 23, no. 9, p. 95007, 2013.

[10] B. D. Jensen, S. Mutlu, S. Miller, K. Kurabayashi, and J. J. Allen, "Shaped comb fingers for tailored electromechanical restoring force," *J. Microelectromechanical Syst.*, vol. 12, no. 3, pp. 373–383, Jun. 2003.

[11] I. I. Izyumin *et al.*, "A 7ppm, 6o/hr frequency-output MEMS gyroscope," in *2015 28th IEEE International Conference on Micro Electro Mechanical Systems (MEMS)*, 2015, pp. 33–36.

[12] Y. Yang, E. J. Ng, Y. Chen, I. B. Flader, and T. W. Kenny, "A Unified Epi-Seal Process for Fabrication of High-Stability Microelectromechanical Devices," *J. Microelectromechanical Syst.*, vol. PP, no. 99, pp. 1–9, 2016.

[13] V. Kaajakari, T. Mattila, A. Oja, and H. Seppa, "Nonlinear limits for single-crystal silicon microresonators," *J. Microelectromechanical Syst.*, vol. 13, no. 5, pp. 715–724, Oct. 2004.

[14] M. Defoort, P. Taheri-Tehrani, and D. A. Horsley, "Exploiting nonlinear amplitude-frequency dependence for temperature compensation in silicon micromechanical resonators," *Appl. Phys. Lett.*, vol. 109, no. 15, p. 153502, Oct. 2016.

[15] C. Guo, E. Tatar, and G. K. Fedder, "Large-displacement parametric resonance using a shaped comb drive," in *2013 IEEE 26th International Conference on Micro Electro Mechanical Systems (MEMS)*, 2013, pp. 173–176.

[16] A. H. Nayfeh and D. T. Mook, *Nonlinear Oscillations*. John Wiley & Sons, 2008.

[17] J. Juillard, A. Bonnoit, E. Avignon, S. Hentz, N. Kacem, and E. Colinet, "From MEMS to NEMS: Closed-loop actuation of resonant beams beyond the critical Duffing amplitude," in *2008 IEEE Sensors*, 2008, pp. 510–513.

CONTACT

*Parsa Taheri-Tehrani, tel: +1-530-341-3080; ptaheri@ucdavis.edu